Hierarchical nano-porous carbon from semi-coke via a MgO template preparation strategy for ONP adsorption

Hongrui Shang, Xinlei Zhang and Junwei Ding*

School of Qingdao University of Science and Technology, Qingdao, China

Abstract. O-Nitrophenol(ONP) industrial wastewater causes serious harm to human body and aquatic environment. In this paper, we adopted a recycled MgO template preparation strategy to design series of semi-coke derived hierarchical porous carbons. The prepared samples were characterized by N_2 adsorption and desorption and scanning electron microscope. The analysis showed that the HPC-1 had a high specific surface area of 723.3m^2 /g with a huge pore volume of 1.64 cm^3 /g and exhibited remarkable adsorption capacity of 503.02 mg/g in batch adsorption test for ONP. Adsorption isotherms and adsorption kinetics revealed the adsorption mechanism of ONP molecules on HPCs surfaces, which followed the langmuir monolayer adsorption and pseudo-second-order kinetic. Furthermore, the HPC-1 exhibited good reusability and recycling performance, reflecting its great potential in practical application.

1. Introduction

Nitro phenolic compounds are an important class of fine chemical products, Playing an important role in today's industrial production[1]. O-Nitrophenol (ONP) is an important intermediate raw material in the manufacture of dyes[2], pesticides[3] and various industrial auxiliaries. However, every coin has two sides, ONP has been listed as one of the 129 toxic chemicals on the Priority Pollutant by the US Environmental Protection Agency (USEPA)[4] because of it's high toxicity and pollution to human body and aquatic environment[5]. The release of these chemical products into the natural environment has a serious impact on water bodies[6]. Therefore, researchers have been trying to find an efficient and low-cost method to remove ONP from water.

Porous carbons has been widely used as adsorbent for removal of organic contaminants from wastewater due to their large specific surface area[7], developed porous structure[8], high thermal stability[9], strong adsorption capacity[9] and extensive sources of raw materials. Semi-coke, a cheap and abundant source of carbon obtained from the low temperature dry distillation of coal[10], usually it costs less than $100 per ton[11]. Therefore, we chose the semi-coke to make high-performance porous carbons.

In recent years, the methods for preparing porous carbons mainly include physical or chemical activation[12]. Physical activation usually uses carbon dioxide[13] or water vapor[14] as the activator, the prepared porous carbons usually have a small specific surface area. Chemiacl activation usually uses KOH[15] or NaOH[16] as the activator. The prepared porous carbon has larger specific surface area and more developed pores. However, the preparation process is activated by corrosive alkali, and it uses excessive activation agents[17], and the activator can not be reused. In addition, the preparation process is complex, usually involving multiple steps such as precursor pretreatment, carbonization and activation. Therefore, in this paper, we have adopted a recyclable template strategy to design series of semi-coke derived porous carbons using magnesium acetate as template precursor, mixing it up by one-pot pyrolysis with simple and feasible operation. And in the process of precursor treatment did not require any organic solvents[18] or hazardous inorganic acids[19], green and pollution-free. For the recycling process of templates, magnesium acetate can be recycled by vacuum evaporation and concentration from the acetic acid pickling solution[20]. Magnesium acetate template precursor can form nano MgO in the pyrolysis process, after the washing process, it can produce a large number of micropores and mesoporous. The obtained porous carbon samples were characterized and applied in the adsorption of the ONP from water to estimate the adsorption properties.

2. Experimental

2.1 A subsection Materials and chemicals

The semi-coke was provied by Daqing Oil Corporation (Heilongjiang, China). Magnesium acetate tetrahydrate [$Mg(CH_3COO)_2{\cdot}4H_2O$] and acetic acid ($CH_3COOH$) were purchased from Sinopharm Chemical Reagent Co., Ltd., Shanghai, O-Nitrophenol (99.5%) used in adsorption evaluation tests was purchased from Aladdin chemical Co., Ltd., Shanghai, China. All chemicals were used as received without further purification. High purity N_2

* Corresponding author: djwnsfc@126.com

(99.999%) was provided by Yantai Deyi Gas Co., Ltd., Shandong, China.

2.2 Synthesis of various porous carbons

HPCs (semi-coke derived hierarchical porous carbons) were prepared by direct carbonization approach using semi-coke as carbon source, $Mg(CH_3COO)_2{\cdot}4H_2O$ as template. In a typical synthesis experiment, 5 g semi-coke powder and 20.10 g $Mg(CH_3COO)_2{\cdot}4H_2O$ (Equivalent to 3.75 g MgO) were added to the mortar and ground to mix well. Subsequently, the fully mixed powder was packed into the corundum boat, transferred into a tube furnace, and heated to 200 ℃ at 5 ℃/min, then heated to 700 ℃ at 1.5
℃/min and kept for 60 minutes under the protection of 45 mL/min N_2 flow to make HPCs. After naturally cooling to room temperature, the carbonized samples were soaked and washed in acetic acid solution to remove the template. They were washed with hot distilled water (75℃) until the pH of the filtrating solution was 7, and then dried in vacuum at 100 ℃ for 24 h to obtain porous carbons. The porous carbons obtained by MgO and semi-coke mass ratio of 0.25, 0.5, 0.75, 1 and 1.25 are defined as HPC-0.25, HPC-0.5, HPC-0.75, HPC-1 and HPC-1.25, respectively.

2.3 Materials characterization

The surface morphology and microstructure of the porous carbon samples were observed via scanning electron microscope (SEM, JSM-7500F, JEOL Ltd.). The pore volumes, pore size distributions and specific surface area of the porous carbon samples were characterized via the N_2 adsorption-desorption method using a Kubo X1000 (Beijing Builder) surface area analyzer.

2.4 Adsorption experiment

In this experiment, the prepared samples were used as the adsorbent, and ONP as the adsorbate. Before the experiments, ONP solutions of different concentrations were prepared ranging from 25 to 500 mg/L. The porous carbon and 50 ml of ONP solution of different concentrations were added to the conical flask, and the conical flask was palced in the shaking bath (HSY-B, Changzhou Zhongbei Instrument Co., Ltd, Changzhou, China), and vibrated at 160 rpm. After adsorption, the porous carbon was filtered. The concentration of ONP in the filtrate was specified through an UV-vis spectrophotometer (UV-3100PC, MAPADA) at 314nm[21].

The equilibrium adsorption (q_e) was calculated by Eq. (1)

$$q_e=\frac{(C_0-C_e)}{m}\times V \quad (1)$$

C_0, and C_e are the initial concentration and equilibrium concentration of the ONP solution (mg/g), respectively. m and V are the weight of carbon adsorbent and the volume of solution, respectively.

The adsorption capacity q_t of ONP at time t can be determined by Eq. (2):

$$q_t=\frac{(C_0-C_t)}{m}\times V \quad (2)$$

where C_t refers to the concentration of ONP at time t.

Adsorption efficiency or percentage removal of ONP was determined by utilizing the following mathematical Eq. (3) :

$$\text{removal}\%=\frac{(C_0-C_e)}{C_0}\times 100 \quad (3)$$

3. Results and Discussion

3.1 Characterization of the prepared porous carbon

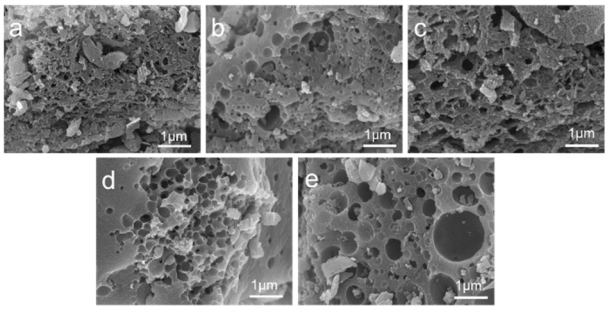

Figure 1. SEM images of (a) HPC-0.25, (b) HPC-0.5, (c) HPC-0.75, (d). HPC-1(e).HPC-1.25.

The SEM images of samples prepared with various mass ratio of MgO to semi-coke are displayed as Fig. 1a to Fig. 1e. When the mass ratio is low, the porous carbon surface has fewer pores (Fig.1a). With the increase of the mass ratio of MgO, the pore structure of carbon materials become more and more developed, which is due to the decomposition of magnesium acetate produces magnesium oxide[22]. After the removal of magnesium oxide by pickling, the porous carbon will appear a hierarchical porous pore structure. In addition, when the mass ratio of MgO to semi-coke is 1, it is found that the pore structure is more developed than the other samples. Continuing to increase the mass ratio, the pore size becomes larger, which may be due to the accumulation of magnesium acetate.

Table 1. Textural characteristics of HPC Samples

Samples	S_{BET} (m^2/g)	V_{Total} [a] (cm^3/g)	V_{Micro} [b] (cm^3/g)	V_{Meso} [b] (cm^3/g)	Average pore diameter (nm)
HPC-0.25	143.15	0.279	0.031	0.248	4.76
HPC-0.5	290.34	0.598	0.045	0.553	5.52
HPC-0.75	487.66	0.913	0.066	0.847	5.48
HPC-1	723.30	1.644	0.068	1.576	7.08
HPC-1.25	646.21	1.389	0.102	1.287	7.50

a Total pore volume adsorbed at P/P_o = 0.9989.
b Calculated by the NLDFT method.

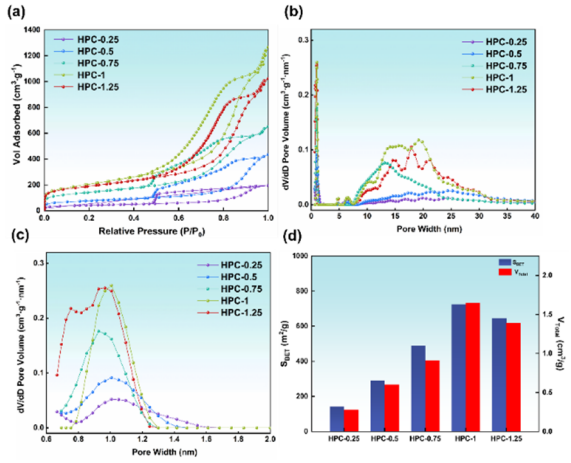

Figure 2. (a) Nitrogen adsorption-desorption isotherms; (b) Pore size distributions (0-40nm) of carbon samples; (c) micropore size distributions of carbon samples; (d) Relationship between specific surface area, total pore volume of materials and mass ratio of MgO to semi-coke.

For the purpose of evaluating the physical properties of the prepared porous carbons, N_2 adsorption-desorption analysis was carried out. The N_2 adsorption-desorption isotherms of various HPCs are shown in Fig.2a. The porous carbons exhibit the same adsorption-desorption isotherms and belongs to type IV classifed by IUPAC[23]. The adsorption of N_2 over HPCs steadily increased as the ratio of MgO increased, but when the mass ratio of MgO template increased to 1.25, the adsorption capacity of N_2 started to decrease. All the samples exhibit rapid adsorption features at the low relative pressure section (P/P_0<0.1), indicating the presence of micropores in the samples[24]. Moreover, in the medium relative pressure range (P/P_0 =0.4-0.9), a obvious adsorption-desorption hysteresis loops close to type H4 appears in the isotherms of all samples, which indicates the co-existence of mesopores and micropores[25]. Fig.2(b, c) shows that the micropores are concentrated at the range of 0.8-1.2nm and the mesopores are focused on the range of 10-30 nm in these HPCs. Undoubtedly, The co-existence of the micropores and mesopores is favorable for transportation and storage, leading to excellent ONP adsorption performance[26].

The detailed pore structure parameters of the carbon samples are summarized in Table 1. As can be seen from Table 1. and Fig.2 (d), the specific surface area of HPCs increase monotonously from 143.15 m^2/g to high specific surface area of 723.30 m^2/g as MgO template to semi-coke mass ratio from 0.25 to 1. Continuing to increase the MgO template could only give rise to a contraction in specific surface area to 646.21 m^2/g, which indicates that magnesium acetate plays an important role in the formation of micropores and mesopores, but too much magnesium acetate will form accumulation and affect the formation of micropores and mesopores.

3.2 Adsorption isotherms

In this study, We use the Langmuir and Freundlich isotherm models to analyze the adsorption data, and there models are given in Eq. (4)(5).

$$q_e = \frac{Q_0 b C_e}{1+bC_e} \quad (4)$$

$$q_e = K_F C_e^{1/n} \quad (5)$$

where Q_0 is the adsorption capacity (mg/g) and b is Langmuir constant (L/mg). where K_F ((mg/g) $(L/mg)^{1/n}$) and n are Freundlich adsorption constants related to the adsorption capacity and adsorption intensity, respectively.

As shown in Fig 3(a, c, e) with the increase of initial concentration, the equilibrium adsorption capacity increases gradually The Langmuir and Freundlich isotherm corresponding parameters were also given in Table 2. In comparison, the R^2 value of the Langmuir isotherm corresponding to the three carbon samples were higher than those of the Freundlich isotherm. This suggests that monolayer adsorption of ONP may occur by porous carbon[27]. Q_0 is the maximum adsorption capacity. It can be seen from Table 2, the maximum adsorption capacity of HPC-0.75 is 525.47 mg/g. HPC-1 and HPC-1.25 are 395.26, 503.02 and 441.88 mg/g, respectively. HPC-1 shows the excellent adsorption ability due to its more adsorption sites.

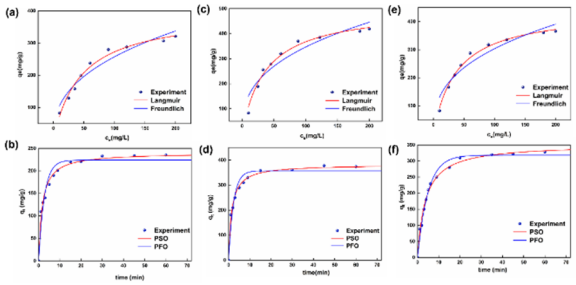

Figure 3. The adsorption equilibrium isotherm fitting curves (a, c and e) and kinetic models fitting curves (b, d and f) of ONP over HPC-0.75, HPC-1 and HPC-1.25.

Table 2. Langmuir and Freundlich isotherm parameters for ONP adsorption

Model	Carbon samples		
	HPC-0.75	HPC-1	HPC-1.25
Langmuir			
Q_0 (mg g^{-1})	395.26	503.02	441.88
b (L mg^{-1})	2.23×10^{-2}	2.27×10^{-2}	2.66×10^{-2}
R^2	0.9825	0.9846	0.9921
R^2_{adj}	0.9801	0.9824	0.9910
Freundlich			
K_f (mg g^{-1})·(L $mg^{-1})^{1/n}$	42.62	65.48	56.73
n	2.56	2.76	2.74
R^2	0.9359	0.9027	0.9210
R^2_{adj}	0.9267	0.8888	0.9096

3.3 Adsorption kinetics

In order to analysis the adsorption mechanism of porous carbons, pseudo first- order (PFO) and pseudo-second-order (PSO) models are used to fit the experimental data, and there models are given in Eq. (6)(7).

$$\log(Q_{e1} - Q_t) = \log Q_{e1} - \frac{k_1}{2.303}t \quad (6)$$

$$\frac{t}{Q_t} = \frac{1}{k_2 Q_{e2}^2} + \frac{t}{Q_{e2}} \quad (7)$$

The fitted parameters were shown in Table.3. As can be seen from it, the correlation coefficient R^2 of the PSO model were higher than those from the PFO under the same conditions. These suggested that the adsorption system studied followed the PSO kinetic model[28]. Which indicated that the adsorption behavior of ONP was not only affected by physical adsorption, but also influenced by the surface chemical species[29, 30]. The fitted curves were shown in Fig.3(b, d, f). Obviously, HPC-1 reached adsorption equilibrium quickly, which might be closely related to the larger pore volume and specific surface area.

Table 3. PSO and PFO kinetic parameters of ONP adsorption onto the prepared carbon samples

Model	Carbon samples		
	HPC-0.75	HPC-1	HPC-1.25
Pseudo-second-order (PSO)			
Q_{e2} (mg/g)	240.17	382.17	352.32
K_2 (g/(mg min))	2.46×10^{-3}	1.82×10^{-3}	7.65×10^{-4}
R^2	0.9863	0.9919	0.9912
R^2_{adj}	0.9851	0.9910	0.9905
Pseudo-first-order (PFO)			
Q_{e1} (mg/g)	223.78	357.30	318.16
K_1(min^{-1})	0.3737	0.4365	0.2054
R^2	0.9435	0.9539	0.9850
R^2_{adj}	0.9384	0.9493	0.9837

3.4 Reusability studies

Reusability is a very important indicator to evaluate the performance of porous carbons, and porous carbon with good reusability can significantly reduce the cost. The HPC-1 was regenerated with ethanol aqueous solution after three consecutive adsorptions. It can be seen from Fig.4, The removal of HPC-1 shows a smoothly decreasing trend as the number of cycles increases. The removal rate remains 93.3% even after the four consecutive reuse-regeneration cycles.

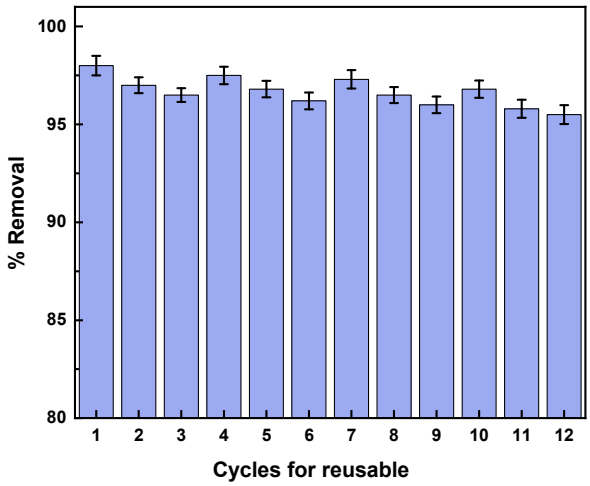

Figure 4. Two or more references. The effects of reuse times of HPC-1 on ONP removal capacity. (Initial concentration of ONP=400 mg/L; equilibrium time=12 h; solution volume=50 mL; adsorbent dosage=0.015 g)

4. Conclusion

The semi-coke was successfully used to synthesize value-added HPCs through a facile one-step "carbonization" strategy using low-template, and successfully applied as an adsorbent for the removal of ONP in wastewater treatment. Magnesium acetate as pore-forming agent can significantly increase the specific surface area of porous carbons and produce hierarchical nano-porous structure. N_2 adsorption-desorption analysis indicated that the HPC-1 had a high specific surface area of 723.3 m^2/g with a huge pore volume up to 1.6 cm^3 /g, exhibiting remarkable adsorption performance to ONP were 503.02 mg/g in batch adsorption test. And the isotherms and kinetic experimental data indicated that adsorption follows Langumir and PSO mechanism. Furthermore, HPC-1 displays excellent reusability and great practical application potential for ONP removal in the reusability test. In summary, this work provided a facile and sustainable approach to mitigate the environmental threat of ONP industrial wastewater, and achieved efficient conversion and utilization of semi-coke.

References

1. Altaher H, Dietrich A M. Characterizing o- and p-nitrophenols adsorption onto innovative activated carbon prepared from date pits [J]. Water Science and Technology, 2013, 69(1): 31-37.
2. Cotoruelo L M, Marqués M D, Díaz F J, et al. Adsorbent ability of lignin-based activated carbons for the removal of p-nitrophenol from aqueous solutions [J]. Chemical Engineering Journal, 2012, 184: 176-183.
3. Ahmaruzzaman M, Laxmi Gayatri S. Batch adsorption of 4-nitrophenol by acid activated jute stick char: Equilibrium, kinetic and thermodynamic studies [J]. Chemical Engineering Journal, 2010, 158(2): 173-180.

4. Kumar A, Kumar S, Kumar S, et al. Adsorption of phenol and 4-nitrophenol on granular activated carbon in basal salt medium: Equilibrium and kinetics [J]. Journal of Hazardous Materials, 2007, 147(1): 155-166.
5. Keerthana M, Pushpa Malini T, Sangavi R. Efficiency of cerium oxide (CeO2) nano-catalyst in degrading the toxic and persistent 4-nitrophenol in aqueous solution [J]. Materials Today: Proceedings, 2021:
6. Akilandaeaswari B, Muthu K. One-pot green synthesis of Au-Ag bimetallic nanoparticles from Lawsonia inermis seed extract and its catalytic reduction of environmental polluted methyl orange and 4-nitrophenol [J]. Journal of the Taiwan Institute of Chemical Engineers, 2021, 127: 292-301.
7. Sun Y, Webley P A. Preparation of activated carbons from corncob with large specific surface area by a variety of chemical activators and their application in gas storage [J]. Chemical Engineering Journal, 2010, 162(3): 883-892.
8. Fu G, Li H, Bai Q, et al. Dual-doping activated carbon with hierarchical pore structure derived from polymeric porous monolith for high performance EDLC [J]. Electrochimica Acta, 2021, 375: 137927.
9. Liu Z, Zang C, Ju Z, et al. Consistent preparation, chemical stability and thermal properties of a shape-stabilized porous carbon/paraffin phase change materials [J]. Journal of Cleaner Production, 2020, 247: 119565.
10. Geng W, Ma F, Wu G, et al. MgO-templated hierarchical porous carbon sheets derived from coal tar pitch for supercapacitors [J]. Electrochimica Acta, 2016, 191: 854-863.
11. He X, Zhang N, Shao X, et al. A layered-template-nanospace-confinement strategy for production of corrugated graphene nanosheets from petroleum pitch for supercapacitors [J]. Chemical Engineering Journal, 2016, 297: 121-127.
12. Zhang W, Cheng R-R, Bi H-H, et al. A review of porous carbons produced by template methods for supercapacitor applications [J]. New Carbon Materials, 2021, 36(1): 69-81.
13. Gunasekaran S S, Badhulika S. High-performance solid-state supercapacitor based on sustainable synthesis of meso-macro porous carbon derived from hemp fibres via CO2 activation [J]. Journal of Energy Storage, 2021, 41: 102997.
14. Lee S M, Lee S H, Jung D H. Surface oxidation of petroleum pitch to improve mesopore ratio and specific surface area of activated carbon [J]. Scientific Reports, 2021, 11(1):
15. Gañan J, González-GarcíA C M, González J F, et al. Preparation of activated carbons from bituminous coal pitches [J]. Applied Surface Science, 2004, 238(1): 347-354.
16. Byamba-Ochir N, Shim W G, Balathanigaimani M S, et al. Highly porous activated carbons prepared from carbon rich Mongolian anthracite by direct NaOH activation [J]. Applied Surface Science, 2016, 379: 331-337.
17. He S, Shi G B, Xiao H, et al. Self S-doping activated carbon derived from lignin -based pitch for removal of gaseous benzene [J]. Chemical Engineering Journal, 2021, 410:
18. Abudu P, Wang L, Xu M, et al. Hierarchical porous carbon materials derived from petroleum pitch for high-performance supercapacitors [J]. Chemical Physics Letters, 2018, 702: 1-7.
19. Shao J, Ma F, Wu G, et al. In-situ MgO (CaCO3) templating coupled with KOH activation strategy for high yield preparation of various porous carbons as supercapacitor electrode materials [J]. Chemical Engineering Journal, 2017, 321: 301-313.
20. Li X, Shan Y, Zhang X, et al. Waste eliminated by waste under COVID-19 pandemic: Mixed plastic waste derived N,O-rich porous carbon nano-coral reefs for chlorophenol pollutants efficient capture [J]. Journal of Environmental Chemical Engineering, 2021, 9(6): 106700.
21. Aldawsari A M, Alsohaimi I H, Hassan H M A, et al. Activated carbon/MOFs composite: AC/NH2-MIL-101(Cr), synthesis and application in high performance adsorption of p-nitrophenol [J]. Journal of Saudi Chemical Society, 2020, 24(9): 693-703.
22. Isa K, Nogawa M. Thermal decomposition of magnesium acetate tetrahydrate under self-generated atmosphere [J]. Thermochimica Acta, 1984, 75(1): 197-206.
23. Yz A, Bzad E, Lc A, et al. Rational design of covalent triazine frameworks based on pore size and heteroatomic toward high performance supercapacitors - ScienceDirect [J]. 2022:
24. Yorgun S, Y?Ld?Z D. Preparation and characterization of activated carbons from Paulownia wood by chemical activation with H3PO4 [J]. Journal of the Taiwan Institute of Chemical Engineers, 2015, 53: 122-131.
25. Kwon H-N, Park G D, Kang Y C, et al. Fabrication of bimodal micro-mesoporous amorphous carbon-graphitic carbon-reduced graphene oxide composite microspheres prepared by pilot-scale spray drying and their application in supercapacitors [J]. Carbon, 2019, 144: 591-600.
26. Li J, Chen X, Gong J, et al. Deep insight into the pore size distribution of N-doped porous carbon materials on electrochemical energy storage and CO2 sorption [J]. Diamond and Related Materials, 2020, 105: 107802.
27. Gao Y, He D, Wu L, et al. Porous and ultrafine nitrogen-doped carbon nanofibers from bacterial cellulose with superior adsorption capacity for adsorption removal of low-concentration 4-chlorophenol [J]. Chemical Engineering Journal, 2021, 420: 127411.

28. Zhang Y, Zheng Y, Yang Y, et al. Mechanisms and adsorption capacities of hydrogen peroxide modified ball milled biochar for the removal of methylene blue from aqueous solutions [J]. Bioresource Technology, 2021, 337: 125432.
29. Zhang P, Li Y, Cao Y, et al. Characteristics of tetracycline adsorption by cow manure biochar prepared at different pyrolysis temperatures [J]. Bioresource Technology, 2019:
30. Yfa B, Lh B, Lw A, et al. Adsorption of sulfonamides on biochars derived from waste residues and its mechanism - ScienceDirect [J]. Journal of Hazardous Materials, 2020: